

Photometric and spectroscopic evolution of the type IIP supernova SN 2004et

D. K. Sahu^{*}, G. C. Anupama[†], S. Srividya, S. Muneer

Indian Institute of Astrophysics, Koramangala, Bangalore 560 034, India

Received / Accepted

ABSTRACT

We present optical photometry and spectroscopy of the type IIP supernova SN 2004et that occurred in the nearby galaxy NGC 6946. The observations span a time range of 8 days to 541 days after explosion. The late time bolometric luminosity and the $H\alpha$ luminosity in the nebular phase indicate that $0.06 \pm 0.02 M_{\odot}$ of ^{56}Ni was synthesised during the explosion. The plateau luminosity, its duration and the expansion velocity of the supernova at the middle of the plateau indicate an explosion energy of $E_{\text{exp}} = 1.20_{-0.30}^{+0.38} \times 10^{51}$ ergs. The late time light curve and the evolution of the [OI] and $H\alpha$ emission line profiles indicate the possibility of an early dust formation in the supernova ejecta. The luminosity of [OI] 6300, 6364 Å doublet, before the dust formation phase, is found to be comparable to that of SN 1987A at similar epochs, implying an oxygen mass in the range $1.5 - 2 M_{\odot}$, and a main sequence mass of $20 M_{\odot}$ for the progenitor.

Key words: supernovae: general - supernovae: individual: SN 2004et - galaxies: individual: NGC 6946

1 INTRODUCTION

Supernovae have been classified mainly based on their spectrum near maximum, the events which show the presence of hydrogen lines have been termed as supernovae type II (SNe II) and those which do not show hydrogen are classified as type I. Type II events are thought to arise from the gravitational collapse of stars more massive than $8 M_{\odot}$. SNe II

* E-mail : dks@crest.ernet.in (DKS)

† E-mail : gca@iiap.res.in (GCA)

have been further divided based on their light curve (Baron, Ciatti & Rosino 1979) as type II-L (linear) and type II-P (plateau). Supernovae type IIP (SNe IIP) are characterized by a plateau of nearly constant luminosity in their light curve, originating because of propagation of a cooling and recombination wave through the supernova envelope.

Hamuy (2003) has shown that SNe IIP form a sequence from low-luminosity, low-velocity, nickel-poor events to bright, high velocity, nickel-rich objects. Further, there is an indication that more massive progenitors produce more energetic explosion and supernovae with greater energies produce more nickel. The direct identification of the progenitor of a few SNe IIP indicates these events arise from stars with masses in the range $\sim 8 - 15 M_{\odot}$ (Smartt et al. 2004, Van Dyk et al. 2003, Li et al. 2006).

SN 2004et was discovered by Moretti on Sept. 27, 2004 in the nearby starburst galaxy NGC 6946, which has already produced seven supernovae during 1917 to 2003. Based on a high resolution spectrum that showed a relatively featureless spectrum with a very broad, low contrast $H\alpha$ emission, Zwitter, Munari & Moretti (2004) classified the supernova as a type II event, which was later confirmed by a low resolution spectrum taken on 2004 Oct 01 by Filippenko et al. (2004). The P-Cygni profile of $H\alpha$ was greatly dominated by the emission component, while the other hydrogen Balmer lines had a more typical P-Cygni profile. The continuum was quite blue, although there was very low flux shortward of 4000\AA . The supernova was detected in the radio frequencies at 22.460 GHz and 8.460 GHz on 2004 Oct 5.128 (Stockdale et al. 2004), suggesting the presence of appreciable circumstellar material around SN 2004et. Based on pre-explosion images of NGC 6946, Li et al. (2005) identified the candidate progenitor as a yellow supergiant with an estimated zero age main sequence mass of $15_{-2}^{+5} M_{\odot}$. The identification of the progenitor was confirmed with post-outburst Hubble Space Telescope images obtained on 2005 May 02 (Li, Filippenko & Van Dyk 2005). This makes SN 2004et one of the few core-collapse supernovae with a directly identified progenitor.

The proximity and brightness of SN 2004et made it an ideal target for an intensive monitoring. We present in this paper the results based on extensive photometric and spectroscopic observations of SN 2004et during $\sim 8 - 541$ days since explosion.

2 OBSERVATIONS AND DATA REDUCTION

2.1 Photometry

SN 2004et was observed with the 2m Himalayan Chandra Telescope (HCT) of the Indian Astronomical Observatory (IAO), Hanle, India, using the Himalaya Faint Object Spectrograph Camera (HFOSC), equipped with a 2048×4096 pixel CCD. The central 2048×2048 region of the CCD used for imaging covers a field of view of 10×10 arcmin, with a scale of $0.296 \text{ arcsec pixel}^{-1}$. The photometric monitoring of SN 2004et, in Bessell *UBVRI* filters (Bessell 1990), began on 2004 September 29, soon after its discovery, and continued until 2006 March 16.

The data were bias subtracted, flat-field corrected and cosmic rays removed adopting the standard manner, using the various tasks available under the IRAF software. Data obtained on photometric nights were calibrated using standard fields (Landolt 1992) and a sequence of local standards in the supernova field (ref. Fig. 1) were used for photometric calibration of the supernova. Table 1 gives the *U, B, V, R, I* magnitudes of the secondary standards averaged over a few photometric nights.

Aperture photometry was performed on the local standards using an aperture of radius determined based on an aperture growth curve. The magnitudes of the supernova and also the local standards were estimated using the profile-fitting method, using a fitting radius corresponding to the full width at half maximum of the stellar profile. The difference between aperture and profile-fitting magnitudes was obtained using the standards and this correction was applied to the supernova magnitude. The supernova magnitudes were calibrated differentially with respect to the local standards listed in Table 1, the final magnitude of the supernova was derived by taking an average of these estimates. The estimated supernova magnitudes and errors are listed in Table 2. The errors in the magnitudes were estimated by combining the fit errors in quadrature with those introduced by the transformation of instrumental magnitudes into the standard system.

2.2 Spectroscopy

The spectroscopic observations of SN 2004et started on 2004 Oct 16 and continued until 2005 Dec 30, corresponding to ~ 25 days to ~ 465 days after explosion. The journal of observation is given in Table 3. All spectra were obtained in the wavelength range $3500\text{--}7000 \text{ \AA}$ and $5200\text{--}9200 \text{ \AA}$ at a spectral resolution of $\sim 7 \text{ \AA}$. A few spectra, in the wavelength range $4000\text{--}8500$

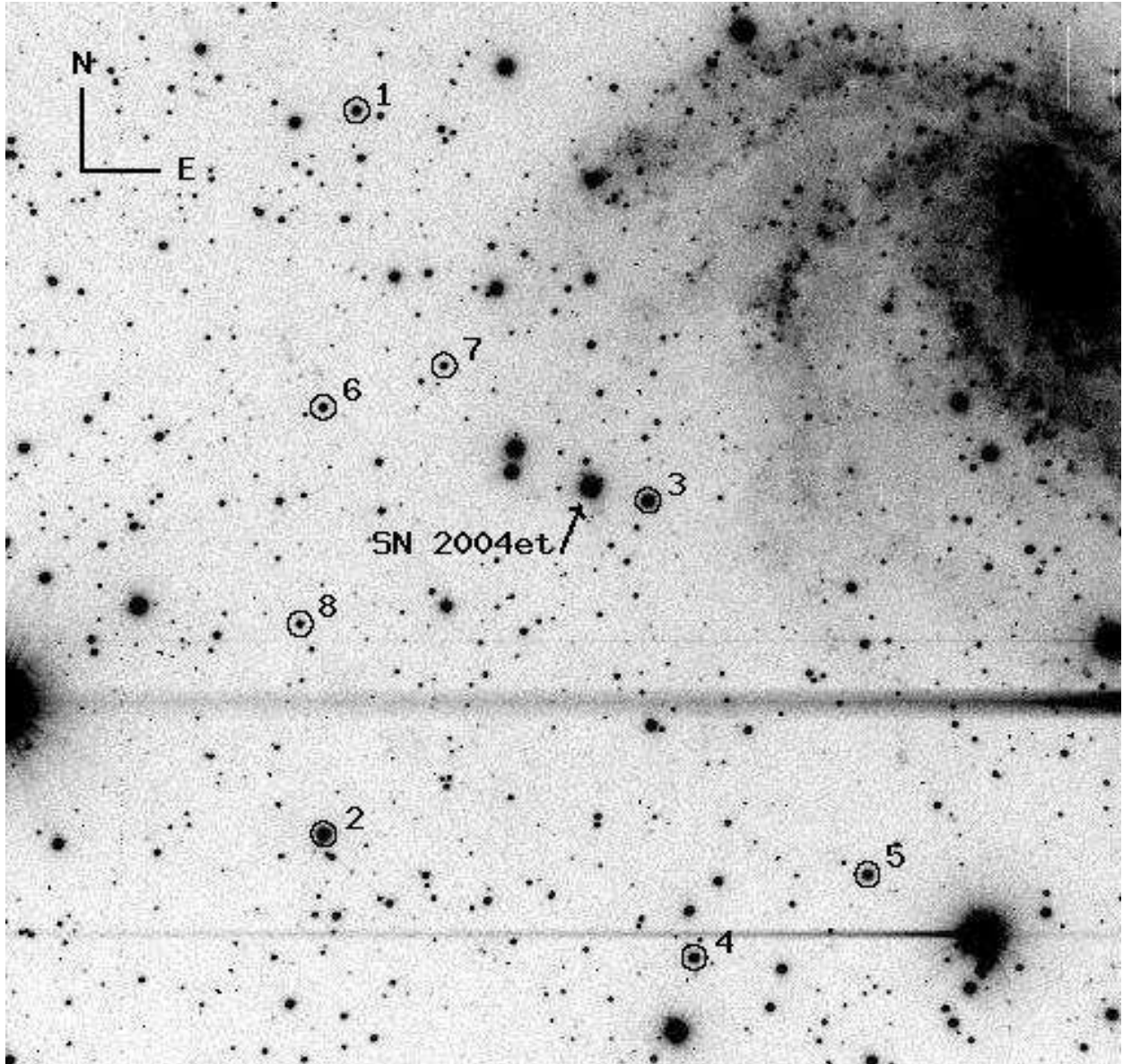


Figure 1. Identification chart for SN 2004et. The stars used as local standards are marked as numbers 1-8. The field of view is $10' \times 10'$.

Table 1. Magnitudes for the sequence of secondary standard stars in the field of SN 2004et. The stars are identified in Fig. 1.

ID	U	B	V	R	I
1	15.927 ± 0.020	15.828 ± 0.008	15.130 ± 0.009	14.672 ± 0.009	14.219 ± 0.009
2	14.439 ± 0.027	14.415 ± 0.010	13.773 ± 0.009	13.353 ± 0.007	12.936 ± 0.011
3	16.665 ± 0.021	15.521 ± 0.010	14.265 ± 0.008	13.568 ± 0.011	12.903 ± 0.008
4	15.840 ± 0.024	15.544 ± 0.017	14.726 ± 0.016	14.255 ± 0.016	13.802 ± 0.009
5	15.780 ± 0.021	15.582 ± 0.012	14.795 ± 0.011	14.336 ± 0.007	13.854 ± 0.008
6	17.485 ± 0.033	16.910 ± 0.012	15.953 ± 0.012	15.399 ± 0.012	14.866 ± 0.009
7	16.957 ± 0.028	16.827 ± 0.015	16.202 ± 0.011	15.782 ± 0.015	15.365 ± 0.025
8	16.865 ± 0.034	16.870 ± 0.017	16.233 ± 0.011	15.842 ± 0.015	15.422 ± 0.015

Table 2. Photometric observations of SN 2004et

Date	J.D. 2453000+	Phase* (days)	U	B	V	R	I
29/09/2004	278.202	7.70	12.308 ± 0.035	12.900 ± 0.018	12.650 ± 0.013	12.360 ± 0.021	
30/09/2004	279.225	8.73	12.224 ± 0.034	12.932 ± 0.026	12.633 ± 0.021	12.331 ± 0.012	
01/10/2004	280.200	9.70	12.254 ± 0.034	12.907 ± 0.017	12.629 ± 0.016	12.314 ± 0.013	
06/10/2004	285.118	14.62	12.418 ± 0.032	12.908 ± 0.012	12.556 ± 0.012	12.216 ± 0.014	12.019 ± 0.018
07/10/2004	286.065	15.57	12.514 ± 0.035	12.921 ± 0.016	12.547 ± 0.013	12.200 ± 0.026	12.009 ± 0.014
09/10/2004	288.059	17.56	12.563 ± 0.038	12.963 ± 0.016	12.549 ± 0.022	12.182 ± 0.018	11.962 ± 0.014
11/10/2004	290.060	19.56	12.673 ± 0.034	12.998 ± 0.017	12.552 ± 0.011	12.156 ± 0.019	11.937 ± 0.019
12/10/2004	291.237	20.74	12.751 ± 0.035	13.047 ± 0.012	12.560 ± 0.019	12.167 ± 0.014	11.927 ± 0.024
13/10/2004	292.077	21.58	12.793 ± 0.033	13.065 ± 0.017	12.558 ± 0.013	12.161 ± 0.020	11.923 ± 0.022
14/10/2004	293.103	22.60	12.885 ± 0.037	13.113 ± 0.021	12.560 ± 0.024	12.160 ± 0.017	11.918 ± 0.019
15/10/2004	294.114	23.61	12.997 ± 0.035	13.162 ± 0.009	12.557 ± 0.019	12.154 ± 0.020	11.922 ± 0.012
16/10/2004	295.125	24.62	13.063 ± 0.046	13.203 ± 0.017	12.568 ± 0.023	12.156 ± 0.015	11.912 ± 0.021
17/10/2004	296.066	25.57	13.178 ± 0.042	13.240 ± 0.013	12.572 ± 0.014	12.157 ± 0.016	11.892 ± 0.018
22/10/2004	301.046	30.55	13.638 ± 0.046	13.501 ± 0.028	12.656 ± 0.020	12.210 ± 0.007	11.916 ± 0.016
23/10/2004	302.045	31.55	13.737 ± 0.043	13.573 ± 0.021	12.646 ± 0.023	12.207 ± 0.021	11.922 ± 0.013
26/10/2004	305.083	34.58	13.865 ± 0.048	13.694 ± 0.026	12.704 ± 0.016	12.249 ± 0.020	11.936 ± 0.019
27/10/2004	306.055	35.55		13.740 ± 0.041	12.687 ± 0.022	12.231 ± 0.020	11.914 ± 0.027
29/10/2004	308.218	37.72	14.195 ± 0.036	13.846 ± 0.027	12.746 ± 0.017	12.247 ± 0.016	11.923 ± 0.021
30/10/2004	309.125	38.62	14.268 ± 0.050	13.867 ± 0.013	12.755 ± 0.023	12.248 ± 0.022	11.929 ± 0.020
01/11/2004	311.132	40.63	14.385 ± 0.033	13.930 ± 0.018	12.767 ± 0.019	12.264 ± 0.008	11.928 ± 0.016
05/11/2004	315.053	44.55	14.623 ± 0.035	14.046 ± 0.019	12.802 ± 0.016	12.283 ± 0.023	11.953 ± 0.031
11/11/2004	321.034	50.53	14.903 ± 0.039	14.197 ± 0.018	12.862 ± 0.029	12.282 ± 0.020	11.934 ± 0.039
12/11/2004	322.067	51.57	14.991 ± 0.034	14.227 ± 0.013	12.848 ± 0.022	12.294 ± 0.016	11.934 ± 0.020
16/11/2004	326.046	55.55	15.180 ± 0.038	14.329 ± 0.016	12.884 ± 0.018	12.310 ± 0.017	11.930 ± 0.014
20/11/2004	330.070	59.57	15.347 ± 0.041	14.408 ± 0.024	12.910 ± 0.023	12.301 ± 0.019	11.927 ± 0.021
24/11/2004	334.072	63.57	15.533 ± 0.041	14.486 ± 0.026	12.942 ± 0.022	12.321 ± 0.022	11.946 ± 0.015
25/11/2004	335.035	64.54	15.568 ± 0.040	14.499 ± 0.024	12.930 ± 0.028	12.317 ± 0.025	11.920 ± 0.019
04/12/2004	344.063	73.56	15.861 ± 0.026	14.657 ± 0.016	12.994 ± 0.024	12.352 ± 0.020	11.946 ± 0.011
08/12/2004	348.041	77.54		14.726 ± 0.013	13.024 ± 0.014	12.371 ± 0.013	11.944 ± 0.019
12/12/2004	352.034	81.53	16.160 ± 0.034	14.788 ± 0.020	13.031 ± 0.013	12.372 ± 0.020	11.957 ± 0.026
16/12/2004	356.096	85.60	16.291 ± 0.034	14.851 ± 0.012	13.075 ± 0.016	12.408 ± 0.018	11.978 ± 0.020
29/12/2004	369.038	98.54		15.118 ± 0.012	13.247 ± 0.024	12.524 ± 0.026	12.093 ± 0.038
06/01/2005	377.044	106.54		15.346 ± 0.011	13.405 ± 0.020	12.651 ± 0.014	12.197 ± 0.022
10/01/2005	381.044	110.54	17.221 ± 0.035	15.522 ± 0.008	13.535 ± 0.013	12.776 ± 0.013	12.296 ± 0.011
13/01/2005	384.043	113.54	17.524 ± 0.040	15.665 ± 0.031	13.660 ± 0.021	12.843 ± 0.022	12.374 ± 0.027
23/01/2005	394.041	123.54		16.527 ± 0.193	14.488 ± 0.117	13.561 ± 0.114	13.005 ± 0.030
07/03/2005	436.511	166.01		17.736 ± 0.069	15.822 ± 0.016	14.735 ± 0.021	14.154 ± 0.019
24/03/2005	454.490	183.99		17.863 ± 0.034	16.002 ± 0.024	14.891 ± 0.022	14.349 ± 0.017
01/04/2005	462.484	191.98			16.117 ± 0.027	14.990 ± 0.012	14.417 ± 0.019
10/04/2005	471.473	200.97				15.048 ± 0.027	
13/04/2005	474.472	203.97		17.961 ± 0.032	16.199 ± 0.013	15.075 ± 0.014	14.527 ± 0.013
15/04/2005	476.469	205.97		17.997 ± 0.037	16.230 ± 0.027	15.102 ± 0.020	14.548 ± 0.020

* Relative to the epoch of date of explosion(JD = 2453270.5)

Å were also obtained with the 1m telescope at the Vainu Bappu Observatory, Kavalur, India, using the UAG spectrograph. All data were reduced using the standard routines within IRAF. The data were bias corrected, flat-fielded and the one dimensional spectra were extracted using the optimal extraction method. The wavelength calibration was done using FeAr and FeNe lamp spectra. The instrumental response curves were obtained using spectrophotometric standards observed on the same night and the supernova spectra were brought to a relative flux scale. On a few nights when the spectrophotometric standards were not observed, the response curves obtained on other nights were used for the flux calibration. The flux calibrated spectra in the two different regions were combined to a weighted mean

Table 2. Table 2 contd.

Date	J.D. 2453000+	Phase* (days)	U	B	V	R	I
21/04/2005	482.403	211.90		18.019 ± 0.035	16.290 ± 0.017	15.152 ± 0.015	14.608 ± 0.020
06/05/2005	497.392	226.89		18.093 ± 0.009	16.436 ± 0.008	15.314 ± 0.009	14.763 ± 0.019
27/05/2005	518.448	247.95		18.260 ± 0.037	16.662 ± 0.023	15.551 ± 0.018	15.016 ± 0.016
28/05/2005	519.385	248.89		18.250 ± 0.018	16.659 ± 0.009	15.538 ± 0.015	15.024 ± 0.021
01/06/2005	523.393	252.89		18.279 ± 0.019	16.705 ± 0.012	15.575 ± 0.009	15.072 ± 0.014
07/06/2005	529.402	258.90		18.322 ± 0.017	16.773 ± 0.012	15.652 ± 0.008	15.127 ± 0.013
20/06/2005	542.419	271.92		18.389 ± 0.019	16.912 ± 0.008	15.792 ± 0.011	15.257 ± 0.016
24/06/2005	546.410	275.91	19.553 ± 0.055	18.414 ± 0.017	16.957 ± 0.017	15.832 ± 0.014	15.336 ± 0.011
25/06/2005	547.418	276.92	19.491 ± 0.055	18.453 ± 0.027	16.975 ± 0.017	15.852 ± 0.016	15.363 ± 0.013
09/07/2005	561.414	290.91	19.630 ± 0.048	18.552 ± 0.020	17.127 ± 0.027	16.018 ± 0.015	15.538 ± 0.012
19/07/2005	571.406	300.91		18.600 ± 0.017	17.245 ± 0.018	16.140 ± 0.013	15.666 ± 0.019
23/07/2005	575.267	304.77	19.526 ± 0.054	18.615 ± 0.018	17.284 ± 0.010	16.183 ± 0.015	15.707 ± 0.020
01/08/2005	584.290	313.79			17.371 ± 0.036	16.298 ± 0.008	15.856 ± 0.016
07/08/2005	590.250	319.75		18.743 ± 0.018	17.446 ± 0.014	16.363 ± 0.014	15.921 ± 0.011
17/08/2005	600.298	329.80		18.836 ± 0.019	17.571 ± 0.014	16.481 ± 0.015	16.059 ± 0.016
23/08/2005	606.235	335.73		18.902 ± 0.023	17.638 ± 0.019	16.563 ± 0.012	16.125 ± 0.016
10/09/2005	624.223	353.72		19.024 ± 0.019	17.831 ± 0.013	16.789 ± 0.011	16.371 ± 0.009
28/09/2005	642.095	371.59	19.982 ± 0.034	19.187 ± 0.018	18.044 ± 0.017	17.024 ± 0.013	16.647 ± 0.020
30/09/2005	644.133	373.63	19.905 ± 0.032	19.182 ± 0.015	18.067 ± 0.009	17.065 ± 0.007	16.667 ± 0.010
17/10/2005	661.207	390.71		19.278 ± 0.078	18.264 ± 0.018	17.254 ± 0.018	16.874 ± 0.027
27/10/2005	671.175	400.67		19.422 ± 0.015	18.376 ± 0.010	17.403 ± 0.012	17.036 ± 0.014
23/11/2005	698.109	427.61		19.680 ± 0.017	18.730 ± 0.016	17.798 ± 0.006	17.426 ± 0.017
26/12/2005	731.103	460.60			19.202 ± 0.016	18.318 ± 0.013	17.919 ± 0.025
06/03/2006	801.493	531.29				19.477 ± 0.027	
16/03/2006	811.426	540.93			20.348 ± 0.041	19.608 ± 0.0265	

* Relative to the epoch of date of explosion(JD = 2453270.5)

to give the final spectrum on a relative flux scale. The spectra were brought to an absolute flux scale using zero points obtained by comparing with the photometric magnitudes. The telluric lines are not removed from the spectra.

2.3 Light Curve

The light curves of SN 2004et in the *UBVRI* bands are plotted in Fig. 2. Based on the non-detection of the supernova, with a limiting magnitude of 19.4 ± 1.2 , on September 22.017 and the subsequent detection at a magnitude of 15.17 ± 0.16 on September 22.983, Li et al. (2005) constrained the date of explosion to be 2004 September 22.0 (JD 2453270.5). Our photometric observations of SN 2004et thus span the range of 8 days (JD 2453278.2) to 541 days (JD2453811.4) since explosion.

A family of cubic spline fits were made to the observed data points around maximum to estimate the date of maximum and maximum magnitude. The dates of maximum and maximum magnitudes were determined as an average of the values of these fits with the uncertainties given by the respective standard deviation of the estimates. The values thus obtained are $m_U(\text{max}) = 12.17 \pm 0.05$ on JD 2453279.93 ± 1.50, $m_B(\text{max}) = 12.89 \pm 0.02$ on JD 2453280.90 ± 2.13, $m_V(\text{max}) = 12.55 \pm 0.01$ on JD 2453286.58 ± 0.50, $m_R(\text{max}) = 12.15 \pm 0.02$

Table 3. Journal of spectroscopic observations of SN 2004et.

Date	J.D. 2453000+	Phase* (days)	Range Å
16/10/04	295.1	24.60	3500-7000; 5200-9200
22/10/04	301.1	30.60	3500-7000; 5200-9200
27/10/04	306.0	35.50	5200-9200
30/10/04	309.1	38.60	3500-7000; 5200-9200
01/11/04	311.2	40.70	3500-7000; 5200-9200
11/11/04	321.0	50.50	3500-7000; 5200-9200
16/11/04	326.1	55.60	3500-7000; 5200-9200
18/11/04	328.1	57.50	4000-8500 [†]
19/11/04	329.2	58.60	4000-8500 [†]
24/11/04	334.0	63.50	3500-7000; 5200-9200
04/12/04	344.1	73.60	3500-7000; 5200-9200
14/12/04	354.0	83.50	3500-7000; 5200-9200
17/12/04	357.0	86.50	3500-7000; 5200-9200
29/12/04	369.1	98.60	3500-7000; 5200-9200
12/01/05	383.1	112.60	3500-7000; 5200-9200
03/03/05	433.5	163.00	3500-7000; 5200-9200
13/03/05	443.5	173.00	3500-7000; 5200-9200
25/03/05	455.4	184.90	3500-7000; 5200-9200
10/04/05	471.4	200.90	3500-7000; 5200-9200
21/04/05	482.4	211.90	3500-7000; 5200-9200
06/05/05	497.4	226.90	3500-7000; 5200-9200
28/05/05	516.3	245.80	3500-7000; 5200-9200
01/06/05	523.4	252.90	3500-7000; 5200-9200
07/06/05	529.4	258.90	3500-7000; 5200-9200
25/06/05	547.4	276.90	3500-7000; 5200-9200
19/07/05	571.4	300.90	3500-7000; 5200-9200
01/08/05	584.3	313.80	3500-7000; 5200-9200
17/10/05	661.2	390.70	3500-7000; 5200-9200
27/10/05	671.1	400.60	3500-7000; 5200-9200
23/11/05	598.1	427.60	3500-7000; 5200-9200
30/12/05	735.1	464.60	3500-7000; 5200-9200

* Relative to the epoch explosion (JD = 2453270.5).

† Observed from VBO, Kavalur.

on JD 2453291.47 \pm 1.81 and $m_I(\text{max}) = 11.91 \pm 0.03$ on JD 2453294.57 \pm 1.37. The B maximum occurred ~ 10 days after the explosion.

The light curves in the $UBVRI$ bands show an initial rise, followed by a plateau in the VRI bands, which extends upto ~ 110 days from the date of explosion. The plateau in the VRI light curves and a decline rate of $\beta_{100}^B = 2.2$ mag in the B light curve over the first 100 days since maximum light establishes that SN 2004et is a type IIP event, since the decline rate for SNe IIP is $\beta_{100}^B < 3.5$ (Patat et al. 1994). After the initial rise to maximum, the U band light curve declines rapidly till ~ 100 days, while the decline in the B band is less steep compared to that of the U band. The V band light curve shows a slowly declining trend in the plateau phase while the light curve in the R and I bands show a nearly constant brightness during the plateau phase.

Following the plateau phase, the V light curve displays a steep decline of ~ 2 mag in ~ 40 days (day ~ 110 to ~ 150 ; JD2453380 to JD2453420). Subsequently, the decline is

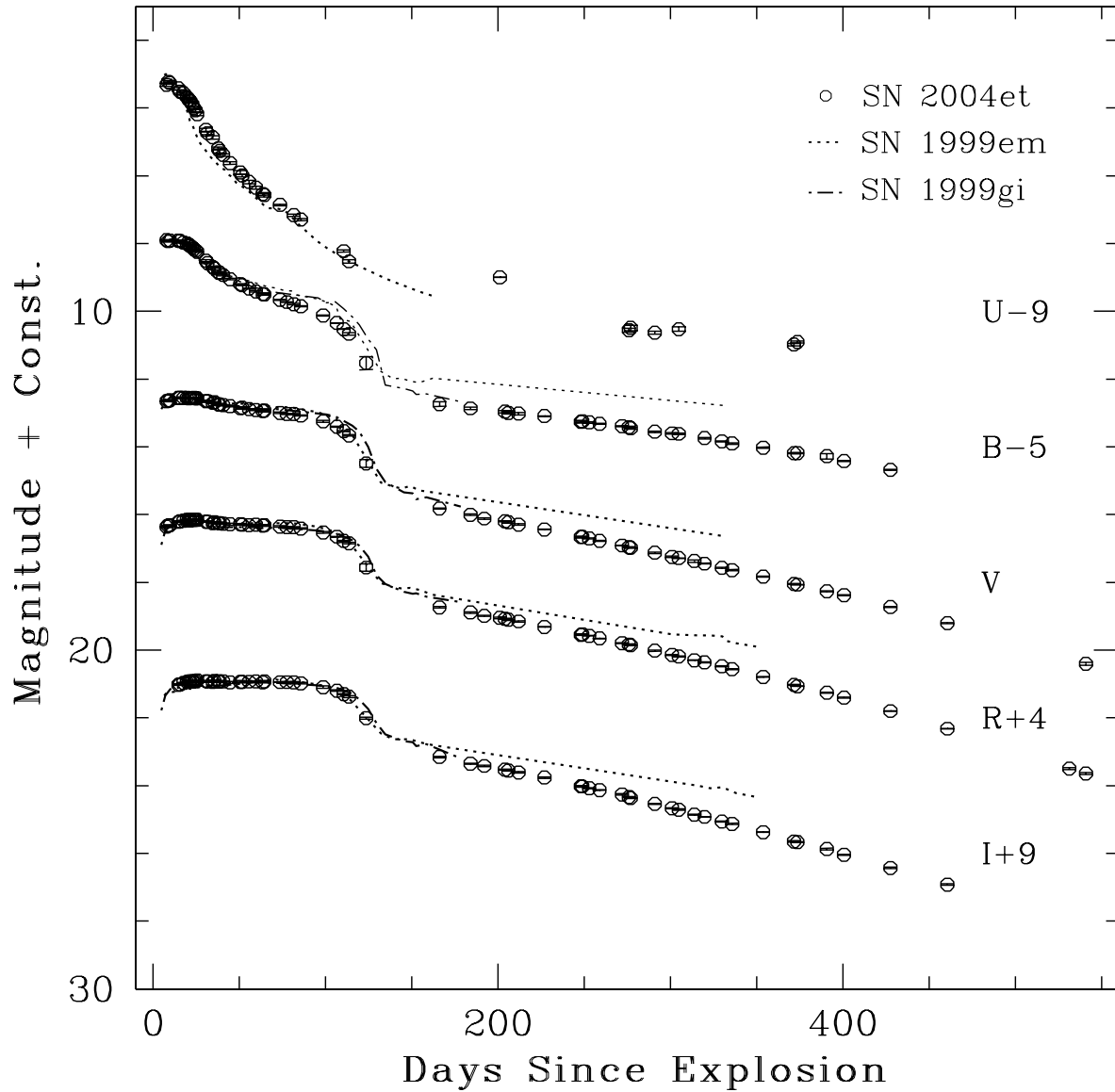


Figure 2. *UBVR* light curve of SN 2004et plotted with other type IIP SNe. Light curves of SN 2004et have been shifted by the reported amounts, other light curves have been shifted by arbitrary amounts to match those of SN 2004et.

linear in all the bands, with decline rates of $\gamma_B \sim 0.64$, $\gamma_V \sim 1.04$, $\gamma_R \sim 1.01$ and $\gamma_I \sim 1.07$, from ~ 180 days to ~ 310 days after explosion. The decline rate steepens beyond 310 days to $\gamma_B \sim 0.84$, $\gamma_V \sim 1.21$, $\gamma_R \sim 1.31$ and $\gamma_I \sim 1.39$. The photometric evolution of SNe IIP at late phases is powered by radioactive decay of ^{56}Co into ^{56}Fe , and the expected decay rate is $\gamma = 0.98 \text{ mag } (100 \text{ d})^{-1}$, especially in the *V* band (Patat et al. 1994). Except for the *B* band, the decay rates obtained during the early nebular phase (180–310 days) are close to that of ^{56}Co decay, suggesting that during this phase γ -ray trapping was efficient. However, the steeper decay rate beyond day 310 indicates that either the supernova had become more

transparent to γ -rays and γ -ray leakage was significant, or dust formation occurred in the supernova ejecta, or it could be a consequence of both the phenomena.

A comparison of the light curves of SN 2004et with those of the well studied SNe IIP, SN 1999em (Leonard et al. 2002a), and SN 1999gi (Leonard et al. 2002b) is made. The *UBVRI* light curves of SN 1999em and SN 1999gi, shifted by arbitrary units in magnitude to match the respective light curves of SN 2004et, are also plotted in Fig. 2. The light curves of all the three SNe are remarkably similar during the early phases. The length of the plateau is also very similar, $\sim 100 - 120$ days for all three events. However, the rate of decline during the nebular phase (beyond day 150) is different; SN 2004et has a steeper decline, indicating a probable difference in the fraction of γ -rays that escape through the supernovae ejecta. It may be noted that the late time photometry of the supernovae are affected significantly by the underlying background of the host, which may flatten the light curve. However, as SN 2004et occurred in the outskirts of the spiral arm, with probably no bright underlying region, background contamination in the late phase is expected to be low, but that may not be the case with SN 1999em and SN 1999gi.

In Fig. 3, we compare the absolute *V* light curve of SN 2004et with those of other SNe IIP, namely, SN 1999em (Leonard et al. 2002a; Hamuy et al. 2001; Elmhamdi et al. 2003), SN 1999gi (Leonard et al. 2002b), SN 1997D (Benetti et al. 2001 and references therein), SN 1990E (Schmidt et al. 1993) and SN 1987A (Hamuy et al. 1988). The supernovae magnitudes have been corrected for extinction using the Cardelli, Clayton & Mathis (1989) extinction law and the following $E(B - V)$: 0.21 for SN 1999gi, 0.10 for SN 1999em, 0.00 for SN 1997D, 0.50 for SN 1990E and 0.15 for SN 1987A. A value of $E(B - V) = 0.41$ is used for SN 2004et (refer Section 4). The distance used to calculate the absolute magnitudes and fluxes are 11.1 Mpc for SN 1999gi (Leonard et al. 2002b), 11.7 Mpc for SN 1999em (Leonard et al. 2003), 13.4 Mpc for SN 1997D (Benetti et al. 2001 and references therein), 21 Mpc for SN 1990E (Schmidt, Krishner & Eastman 1992) and 0.0468 Mpc for SN 1987A (Hamuy et al. 1988). A distance of 5.6 Mpc is used for SN 2004et (refer Section 4). Distance estimates for SN 1990E and SN 1999gi are based on the expanding photosphere method (EPM), SN 1999em distance estimate is based on Cepheid variables (Leonard et al. 2003). For SN 1999em Cepheid distance is nearly 50% greater than the values derived using the EPM. The major source of discrepancy between the distances based on EPM and Cepheid may be attributed to the underestimate of the theoretically derived dilution factors used in

EPM analysis, however, other sources of statistical and systematic uncertainty can not be neglected.

The shape of the light curves of SN 2004et, SN 1999em and SN 1999gi are very similar and the length of the plateau is also almost the same. The absolute magnitude of SN 2004et is similar to that of SN 1990E and is brighter than the other SNe IIP compared here. The average absolute V magnitude during the plateau phase, estimated by taking the unweighted mean of the magnitudes from 20 to 100 days after the explosion is -17.14 for SN 2004et, -15.97 for SN 1999gi and -16.69 for SN 1999em.

The reddening corrected $(U - B)$, $(B - V)$, $(V - R)$ and $(R - I)$ colour curves of SN 2004et are shown in Fig. 4. Also shown in the same figure, for comparison, are the respective colour curves of SN 1999em, SN 1999gi and SN 1990E. There is a noticeable difference in the colour evolution of SN 2004et with those of other SNe IIP in comparison. As noted by Li et al. (2005), during the first month the $(U - B)$ and $(B - V)$ colours of SN 2004et evolve more slowly compared to SN 1999em, the same trend continues till ~ 150 days since explosion. During this period the overall colours of SN 2004et are bluer compared to the other SNe IIP. Beyond ~ 200 days after explosion, the $(B - V)$ and $(V - R)$ colours of SN 2004et are similar to the other SNe IIP. The $(R - I)$ colour is bluer compared to SN 1999em even beyond day 200.

3 SPECTROSCOPY

3.1 Spectroscopic evolution

The spectroscopic evolution of SN 2004et in the rest frame of the SN is displayed in Fig. 5 and Fig. 7. All the spectra have been Doppler corrected for the recession velocity of the host galaxy, taken as 45 km sec^{-1} (Sandage & Tammann 1981). Our first spectrum corresponds to ~ 25 days after explosion. The spectrum has a blue continuum with well developed P-Cygni profiles of hydrogen Balmer lines (upto $H\epsilon$). The $H\alpha$ line is emission dominated with a shallow P-Cygni profile, which appears to consist of two components. The second, high velocity absorption component is shown marked A in Fig. 5. Apart from the hydrogen Balmer lines, CaII (H & K) lines $3934, 3968 \text{ \AA}$, FeII 5169 \AA and the CaII IR triplet $8498, 8542, 8662 \text{ \AA}$ are clearly seen in the spectrum. Interstellar NaI D absorption features at $5890, 5896 \text{ \AA}$ are also present. By day 39, NaI D absorption lines, FeII lines $4924, 5018, 5535 \text{ \AA}$, ScII line 5527 \AA and other blends of FeII, ScII, BaII start appearing. Fig. 6 shows the

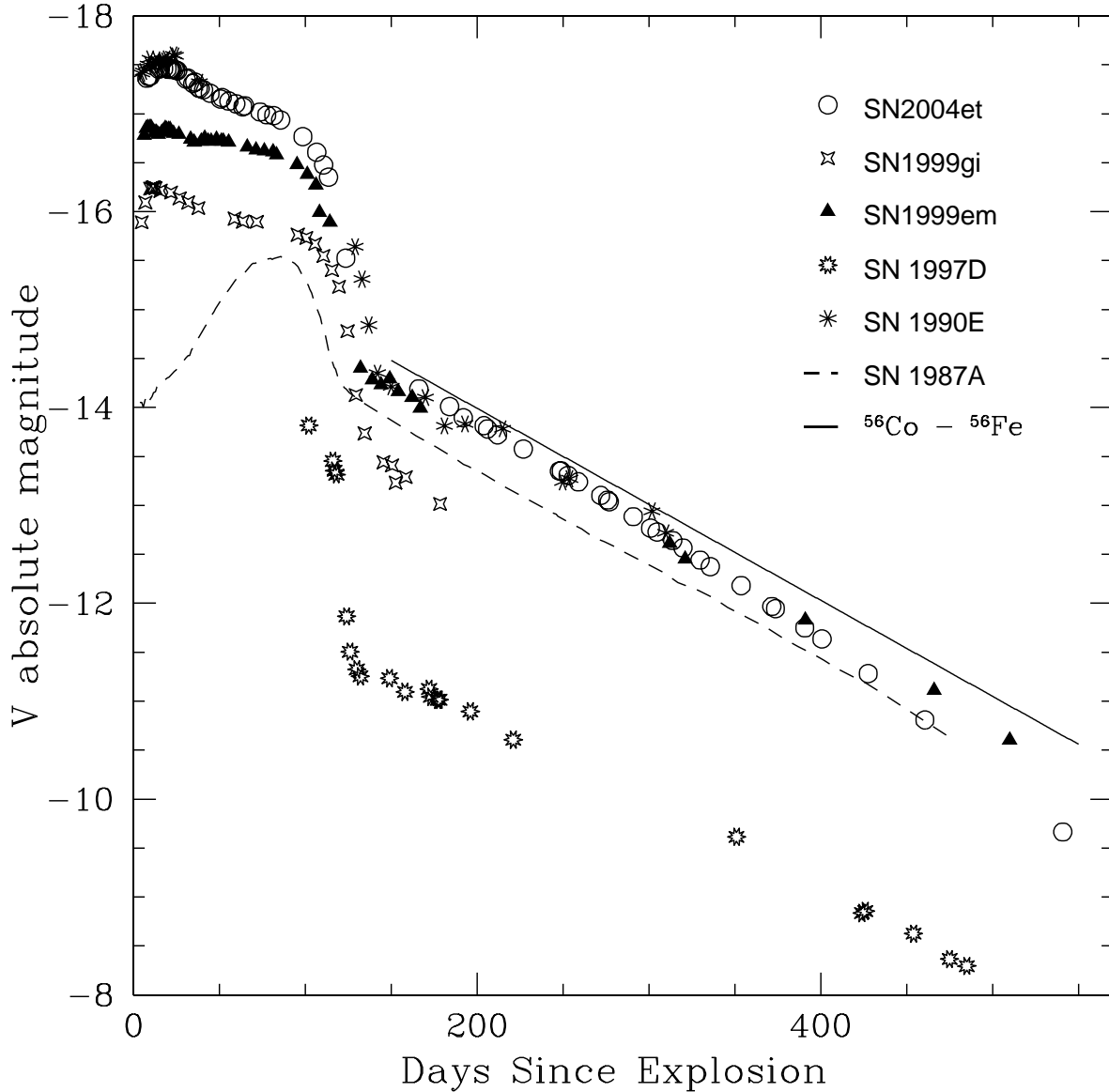


Figure 3. Absolute V light curve of SN 2004et along with those of other SNe IIP. The slope of ^{56}Co to ^{56}Fe radioactive decay is also shown.

spectrum taken 63 days after the explosion, with line identification following Leonard et al. (2002a). In the later phase, ~ 74 days after explosion, except for $\text{H}\alpha$ and $\text{H}\beta$, the Balmer lines are obscured by metal lines.

The two-component P-Cygni profile of $\text{H}\alpha$ noted by (Li et al. 2005) in a spectrum obtained 20 days after the explosion, is clearly seen in our spectrum of day ~ 25 . This feature was present until ~ 113 days, until the end of the plateau phase. This feature was also present in the spectrum of SN 1999em and has been identified as a high velocity component of $\text{H}\alpha$ (Leonard et al. 2002a). Similar high velocity component features are noticed in the

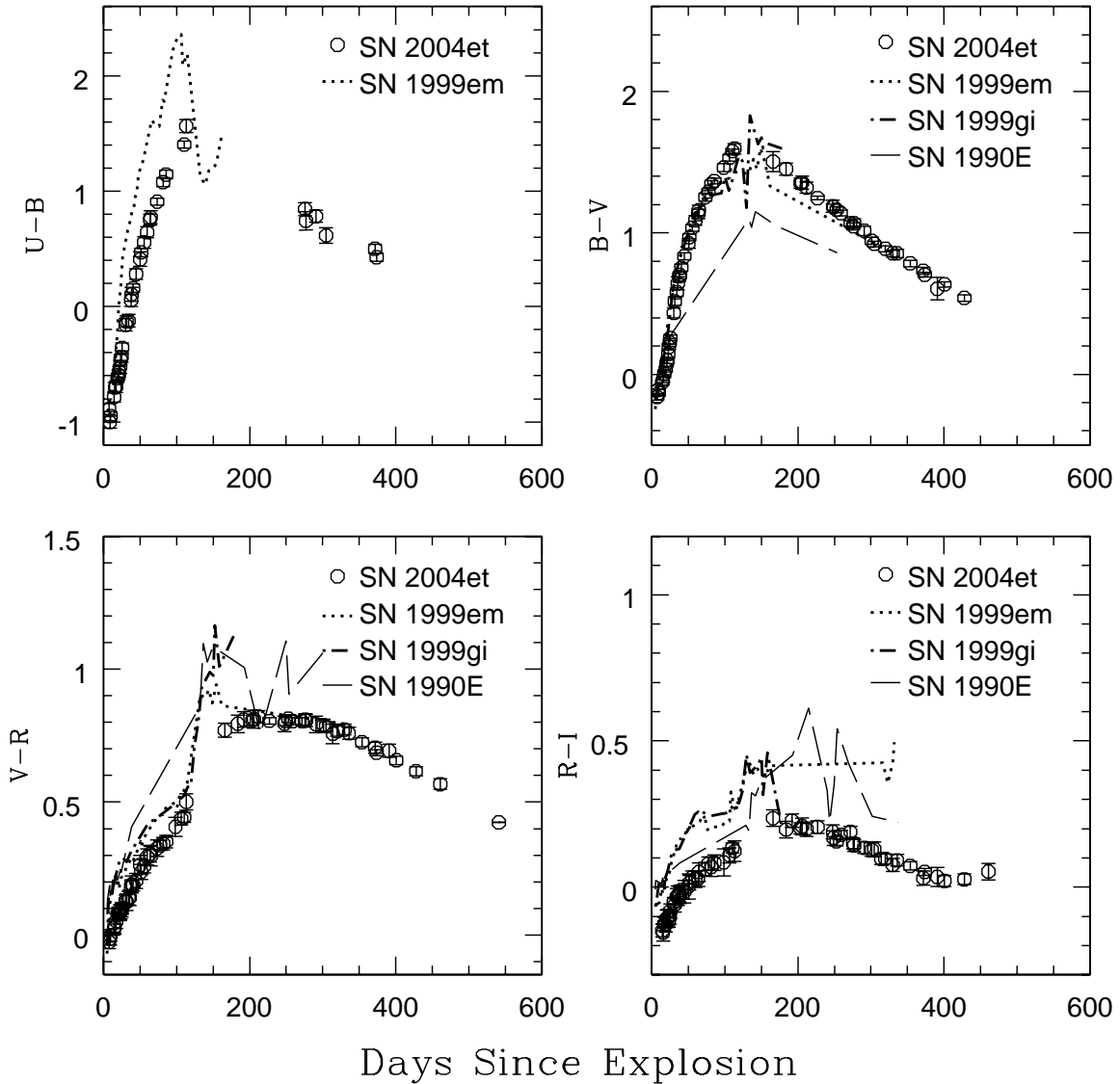


Figure 4. Colour curves of SN 2004et compared with other SNe IIP

$H\beta$ and Na I lines also. These high velocity components could be arising due to interaction of the supernova ejecta with the pre-supernova circumstellar material. Baron et al. (2000) interpret the double component P-Cygni profiles as being produced by a combination of the usual wide P-Cygni profile and a second P-Cygni profile with a highly blueshifted absorption, corresponding to two line forming regions in the expanding atmosphere of the supernova.

As the supernova ages, the absorption components of $H\alpha$, $H\beta$ and the CaII IR triplet become narrower and deeper. In the blue region of the spectrum numerous metal lines due to Fe, Sc, Ba and Sr appear and the emission line strength increases with time till the supernova

enters into the nebular phase. The spectrum obtained ~ 113 days after the explosion is still dominated by absorption features due to metal lines, indicating that the supernova had not yet entered into the nebular phase. However, forbidden lines due to oxygen [O I] 6300, 6364 Å, iron [Fe II] 7155 Å, calcium [Ca II] 7291, 7324 Å start appearing in the spectrum. The spectrum obtained ~ 163 days after explosion shows a significant evolution compared to day 113. The spectrum is more emission dominated, featuring the onset of the nebular phase. In this spectrum, the $H\alpha$ profile has narrowed down and the nebular emission lines of [O I] 6300, 6364 Å and [Ca II] 7291, 7324 Å are well developed.

In the spectra of day 391 and later, the [Ca II] 7291, 7324 Å line is strong compared to $H\alpha$, a feature noticed in the spectrum of SN 1999em around the same epoch (Elmhamdi et al. 2003), but not detected in the SNe IIP, SN 1990E (Benetti et al. 1994), SN 1997D (Benetti et al. 2001 and references therein) and SN 2003gd (Hendry et al. 2005). Fig. 8 shows the luminosity evolution of the nebular lines, $H\alpha$ and [O I] 6300, 6364 Å for SN 2004et. Also shown in the same figure, for a comparison, are the corresponding luminosities for SN 1987A at similar epochs. The nebular line luminosities of SN 2004et before day 300 are similar to SN 1987A. Beyond day 400, SN 2004et lines have lower luminosities.

3.2 Expansion velocity of SN 2004et

The photospheric velocity of the ejecta can be estimated from the minimum of the absorption feature of weak, unblended lines. Hamuy et al. (2001) have shown that the use of Fe II (multiplet 42) at 4924, 5018, 5169 Å provides a good estimate of the photospheric velocity during the plateau phase. As the supernova ages, it becomes difficult to define the minimum of Fe II 5169 Å line and hence the velocity measurement using this line is not a good estimate at these phases. The photospheric velocity estimated using these lines is plotted in Fig. 9. The velocity estimated using the Fe II 4924 Å line (ref. Fig. 9) is lower due to the blending of this line with Ba II 4934 Å (Hendry et al. 2005).

Also plotted in the Fig. 9 are the velocities determined using the absorption minima of $H\alpha$, $H\beta$, and the high velocity component of $H\alpha$. These velocity estimates are higher due to higher optical depths. The evolution of the high velocity component of $H\alpha$ is similar to that of normal component. A comparison of the photospheric expansion velocity determined for SN 2004et, using the weak unblended iron lines, with those of SN 1999em (Hamuy et al. 2001) and SN 1999gi (Leonard et al. 2002b) indicates that SN 2004et has a higher expansion

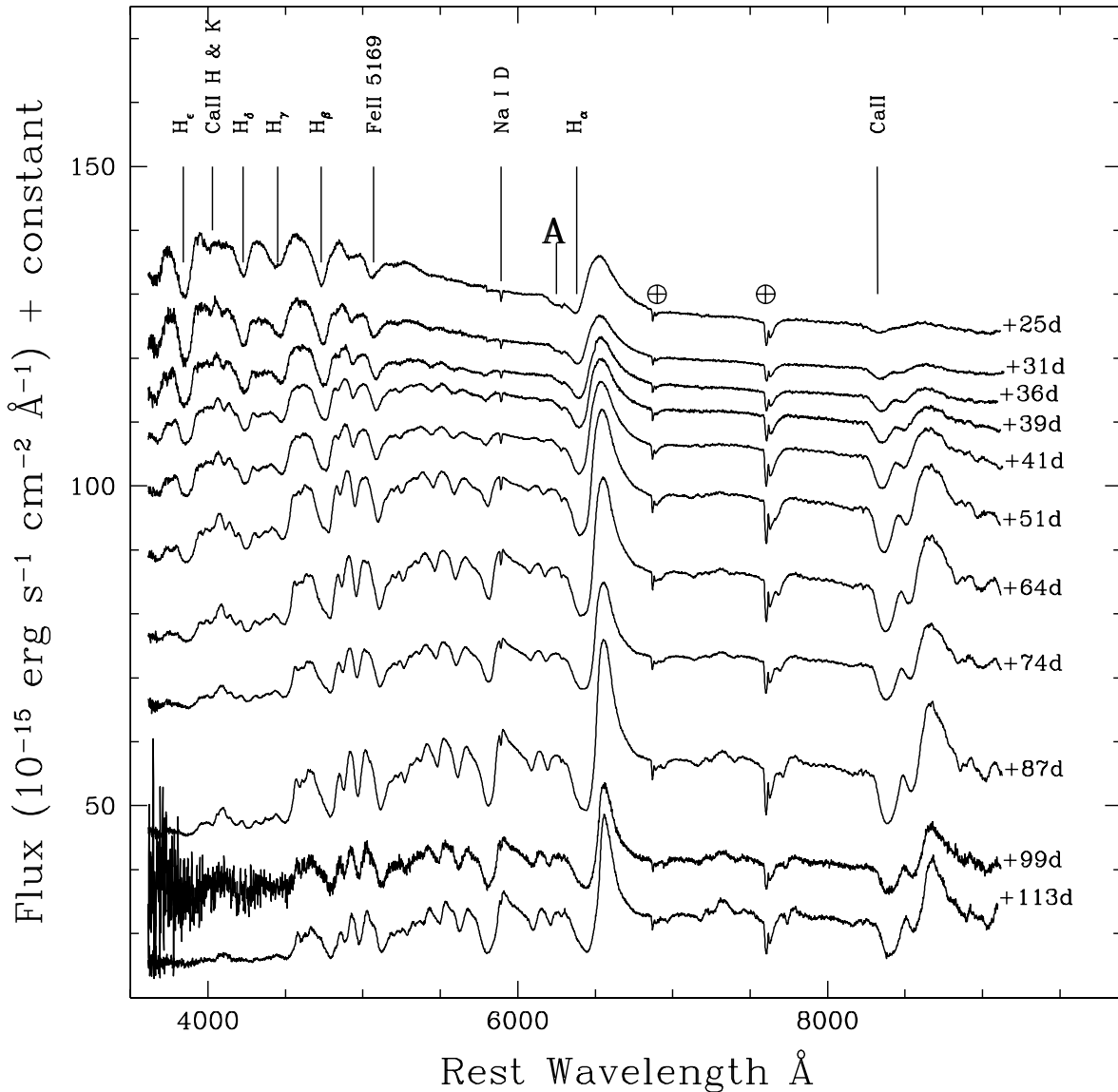


Figure 5. Spectral evolution of SN 2004et during plateau phase.

velocity at similar epochs. For further analyses, we use the average photospheric velocity estimated using the weak iron lines.

4 REDDENING AND DISTANCE ESTIMATES

The interstellar Na lines are clearly seen in the spectra presented here. The equivalent width of the Na I D lines measured from the spectra presented here is 1.70\AA , which corresponds to a total reddening of $E(B - V) = 0.43$ mag, following the empirical relation by Barbon et al. (1990). This estimate is consistent with the estimate by Zwitter, Munari & Moretti (2004)

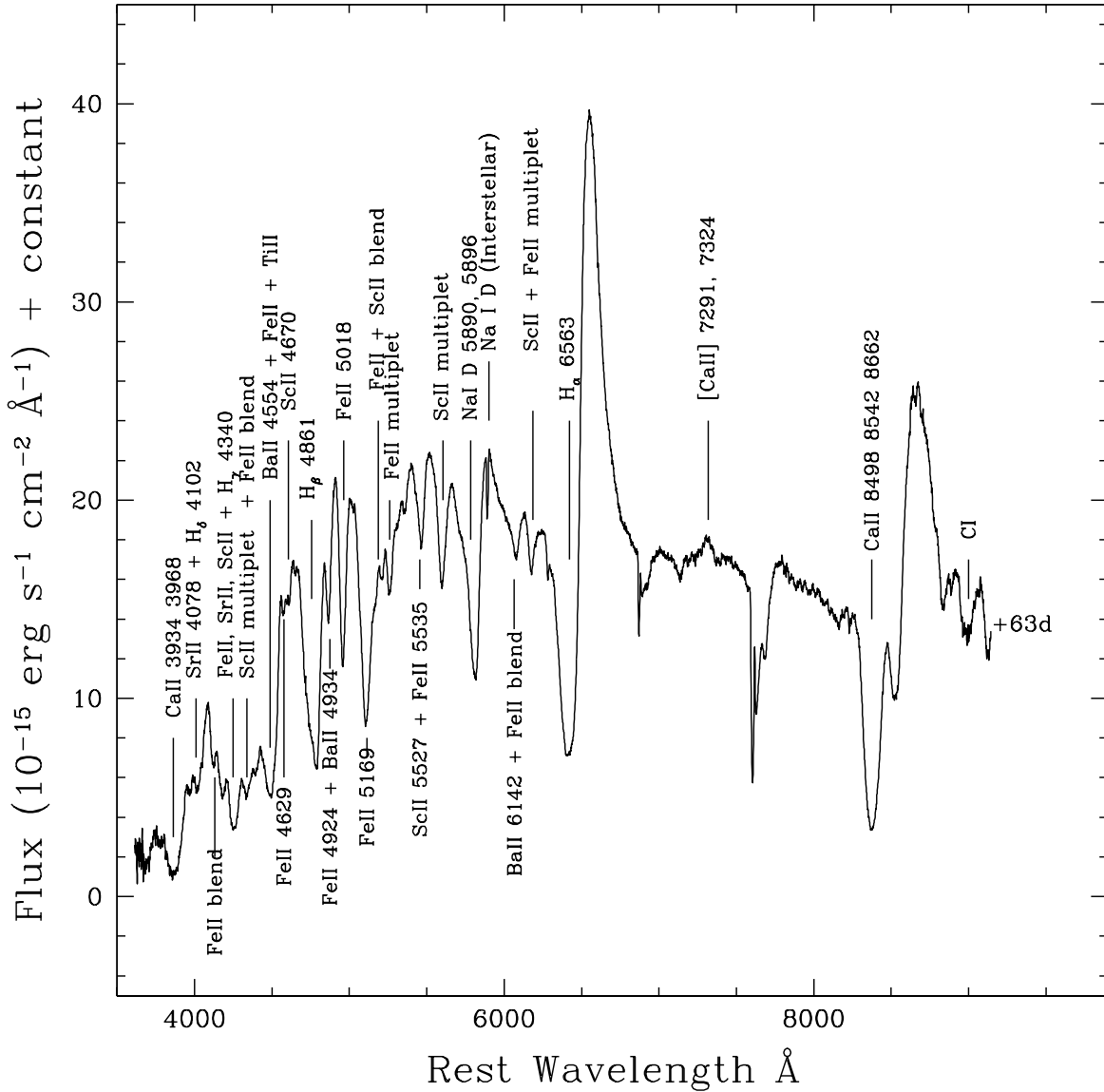


Figure 6. Spectral line identification in plateau phase.

based on equivalent widths of the Na I lines in a high resolution spectrum. The Galactic reddening in the direction of NGC 6946 is $E(B - V) = 0.34$ mag (Schlegel, Finkbeiner & Davis 1998), which implies that the supernova has suffered minimal extinction in the host galaxy. We use $E(B - V) = 0.41$ (Zwitter, Munari & Moretti 2004) mag as the total reddening for further analysis.

The HI Tully Fisher relation (Pierce 1994) indicates a distance of 5.5 Mpc to NGC 6946, while the CO Tully Fisher relation (Schoniger & Sofue 1994) indicates a distance of 5.4 Mpc. The “expanding photosphere method” for the IIP supernova SN 1980K that occurred

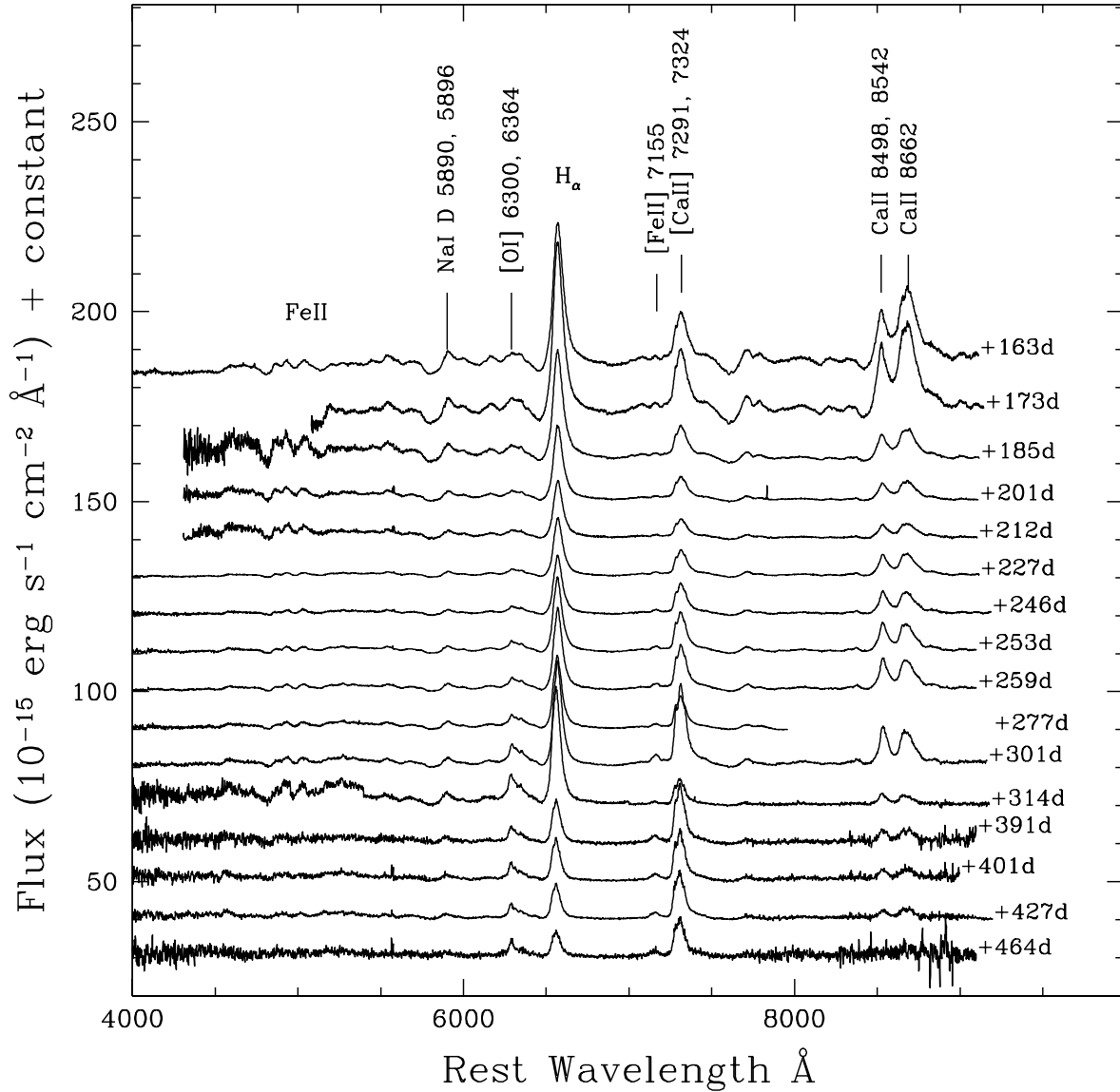


Figure 7. Spectral evolution of SN 2004et in the nebular phase.

in NGC 6946 (Schmidt et al. 1994) yields a distance of 5.7 Mpc. Hamuy & Pinto (2002) have shown that the expansion velocities of the ejecta of SNe IIP are correlated with their bolometric luminosities during the plateau phase. Based on this correlation they establish a “standard candle method (SCM)” to estimate the distance to the supernovae. Nugent et al. (2006) proposed a refinement to the SCM method by introducing the use of $(V - I)$ colour during the plateau phase at day 50 to perform extinction correction rather than relying on colours at the end of the plateau. Using equation 1 of Nugent et al. (2006), with the fitting parameters for low redshift SNe IIP and the observed expansion velocity at day 50

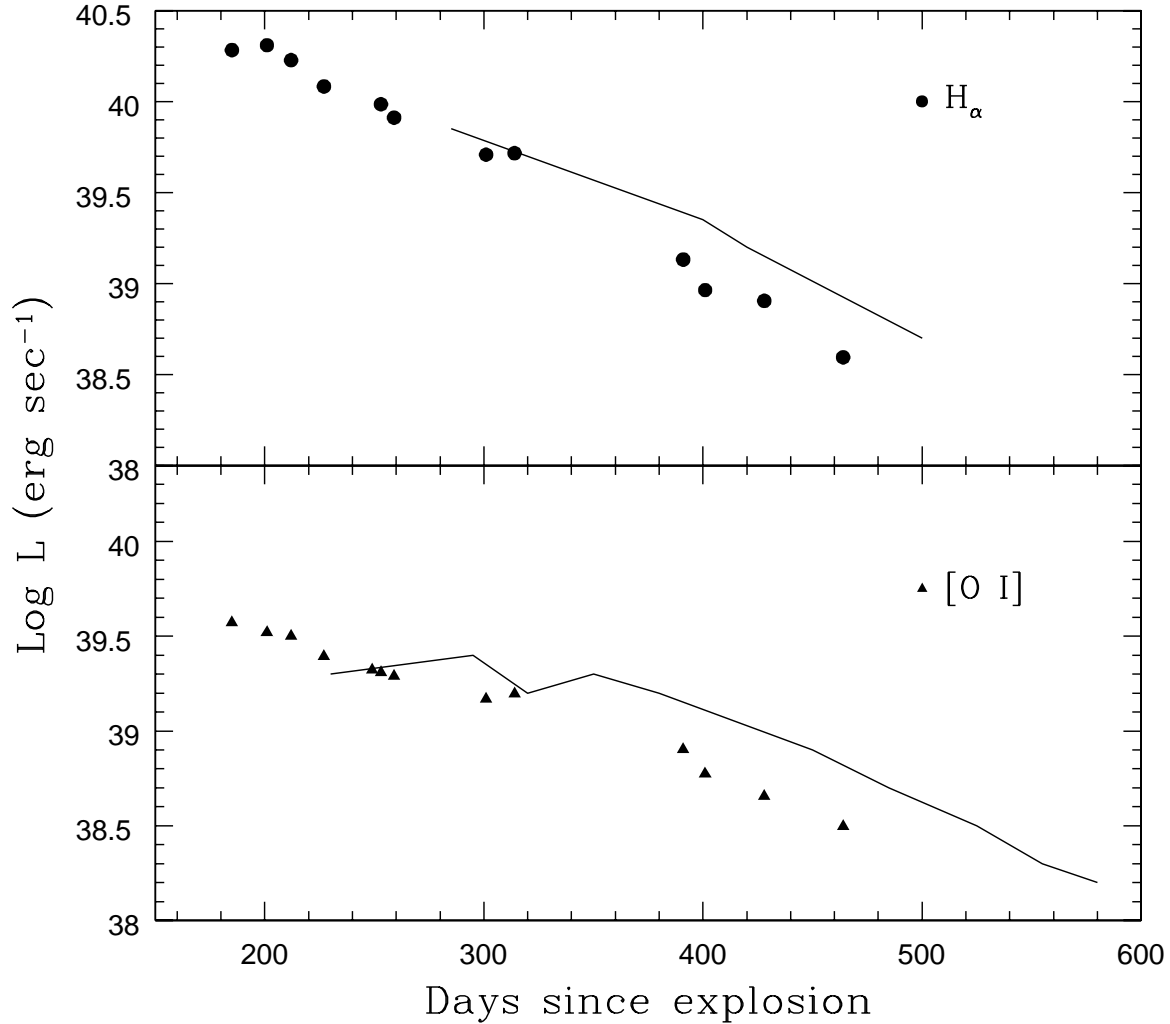


Figure 8. The temporal evolution of the luminosity of nebular lines H α and [O I] for SN 2004et, overplotted curve corresponds to SN 1987A.

$v_{50} = 4122 \pm 170 \text{ km sec}^{-1}$ we estimate the distance to SN 2004et as $5.7_{-0.3}^{+0.3}$ Mpc. Based on all the estimates, an average distance of 5.6 Mpc is assumed for SN 2004et.

5 *UBVRI* BOLOMETRIC LIGHT CURVE AND ^{56}Ni MASS

5.1 *UBVRI* bolometric light curve

The *UBVRI* photometry presented in Section 2.3 is used to derive the *UBVRI* bolometric light curve of SN 2004et. The optical magnitudes have been corrected for reddening values

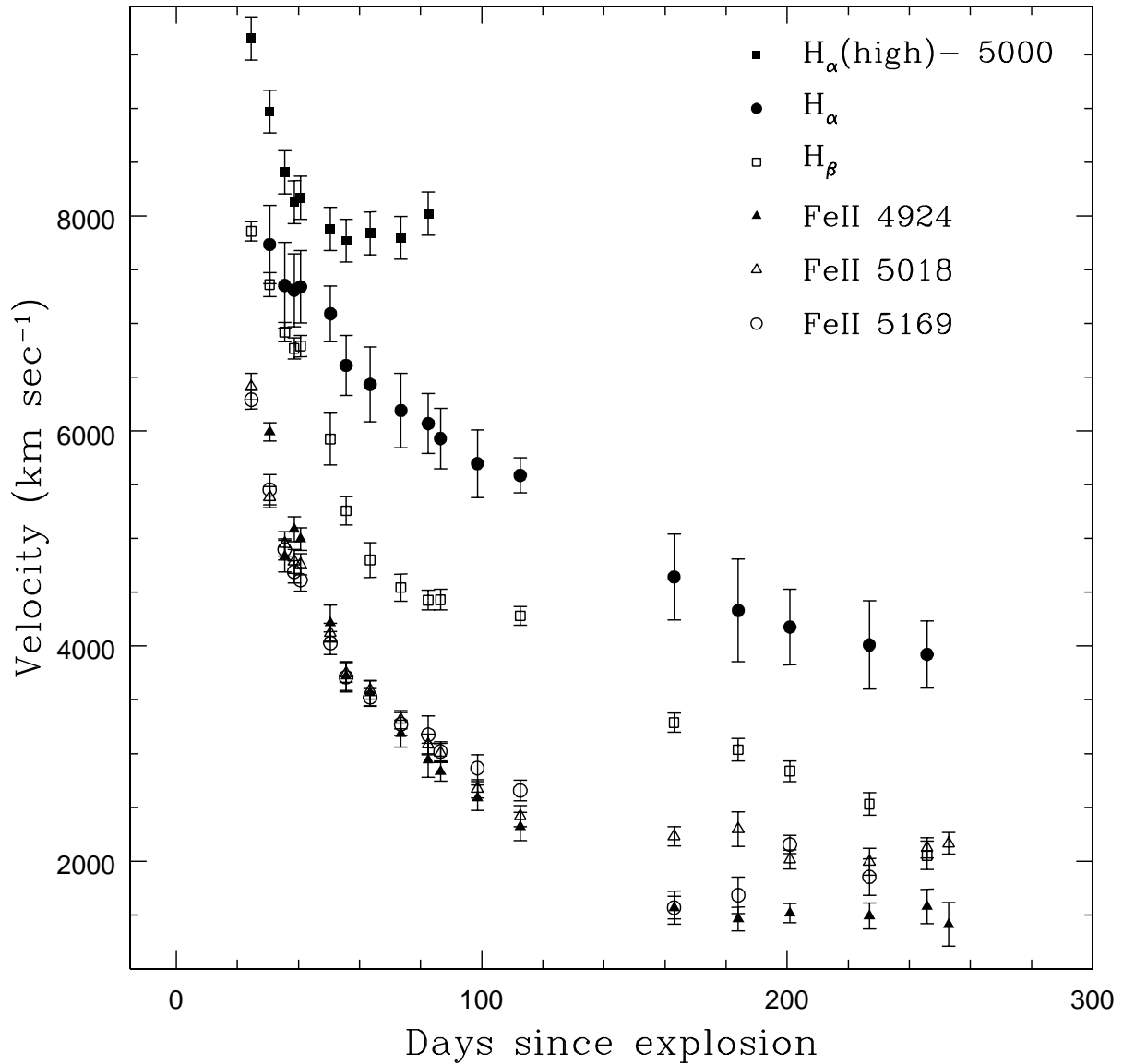


Figure 9. Velocity evolution of SN 2004et

mentioned in Section 2.3 using Cardelli, Clayton & Mathis (1989) extinction law, the corrected magnitudes are then converted to fluxes according to Bessell, Castelli & Plez (1998). The *UBVRI* bolometric fluxes were derived by fitting a spline curve to the *U, B, V, R* and *I* fluxes and integrating it over the wavelength range 3200Å to 10600Å, determined by the response of the filters used. There are some gaps in the *U* band light curve specially after the plateau; the missing magnitudes were obtained by interpolation. In the later stage, however, the light curve is linearly extrapolated to get the missing magnitudes in the *U* band. No corrections have been applied for the missing fluxes in the ultra-violet and the near infra-red

region. Fig. 10 shows the *UBVRI* bolometric light curve of SN 2004et. Also plotted in the same figure are the *UBVRI* bolometric light curves of SN 1999em, SN 1999gi, SN 1997D and SN 1990E. The *UBVRI* bolometric light curve for SN 1990E is taken from the literature (Schmidt et al. 1993), while for other supernovae the *UBVRI* bolometric luminosities are derived from the photometry reported in the references cited in Section 2.3. Since no *U* band magnitudes were available for SN 1999gi and SN1997D the contribution of the *U* flux to the total *UBVRI* flux was assumed to be similar to SN 1999em and SN 2004et. A comparison of the *UBVRI* bolometric light curve of SN 2004et with the other SNe IIP indicates SN 2004et had a higher luminosity. The luminosity during the initial phases is very similar to SN 1990E but its considerably lower in the post-plateau decline.

5.2 ^{56}Ni mass

For most SNe IIP, the early (150-300d) bolometric luminosity on the radioactive tail is equal to the luminosity of the radioactive decay of ^{56}Co . The mass of ^{56}Ni synthesized during the supernova explosion can thus be estimated from the late time bolometric light curve. In absence of infra-red photometry for SN 2004et, we followed Hamuy (2003), to estimate the tail bolometric luminosity L_t , using the *V* magnitudes during the nebular phase and a bolometric correction of 0.26 mag. The tail luminosity is then used to estimate the nickel mass using equation 2 in Hamuy (2003). Based on the luminosity of SN 2004et during 250 to 315 days, estimated using the *V* magnitudes, we estimate the ^{56}Ni mass to be $0.060 \pm 0.02 M_{\odot}$.

Elmhamdi, Chugai & Danziger (2003) find a correlation with the ^{56}Ni mass and the rate of decline in the *V* band light curve from the plateau to the tail. The maximum gradient during the transition from plateau to nebular phase, defined by a steepness parameter $S = dM_V/dt$, is found to anticorrelate with ^{56}Ni mass, in the sense that the steeper the decline at the inflection, the lower is the ^{56}Ni mass. Using a sample of 10 SNe IIP, Elmhamdi, Chugai & Danziger (2003) derive the following relation

$$\log \left(\frac{M_{\text{Ni}}}{M_{\odot}} \right) = -6.2295 S - 0.8147 \quad (1)$$

An accurate determination of the steepness parameter S requires a well sampled *V* band light curve during the end of plateau to the beginning of the radioactive tail. Unfortunately, we do not have a very well sampled light curve during this phase. However, with the available points, we estimate the steepness parameter S as 0.062 ± 0.02 . Using this, the mass of ^{56}Ni

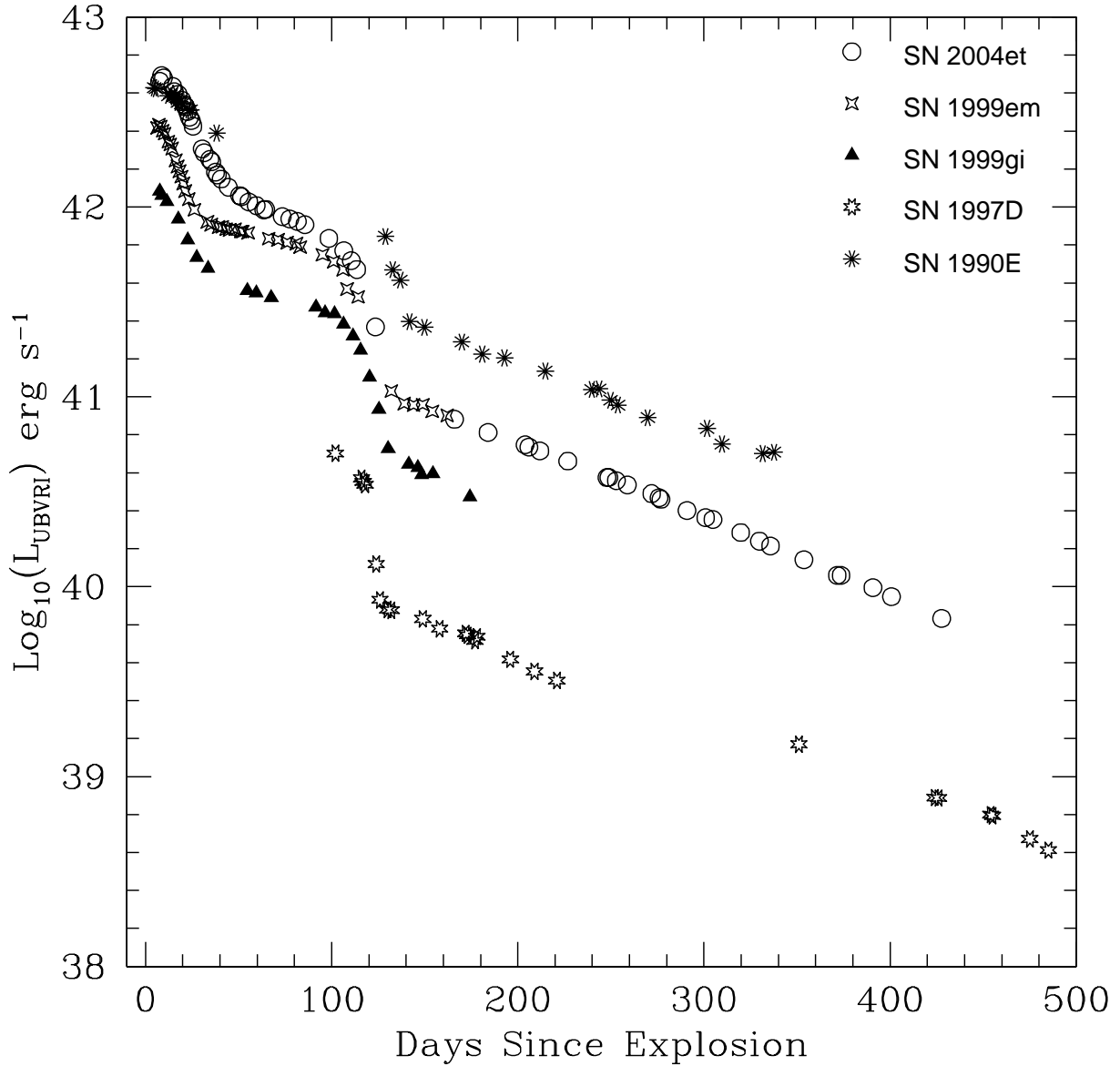


Figure 10. Comparison of *UBVRI* bolometric light curve of SN 2004et with those of other type IIP SNe.

is found to be $0.062 \pm 0.02 M_{\odot}$, which agrees very well with the ^{56}Ni mass derived from *V* magnitude on the radioactive tail.

The nickel mass may also be estimated comparing the bolometric light curve of SN 2004et with that of SN 1987A, assuming that the γ -ray deposition for SN 2004et is the same as that for SN 1987A. The tail bolometric luminosity of SN 2004et ($\sim 250 - 300$) is found to be ~ 1.6 times fainter than that of SN 1987A. This implies a ^{56}Ni mass of $0.048 \pm 0.01 M_{\odot}$ for SN 2004et, for a value of $0.075 M_{\odot}$ for SN 1987A (Turatto et al. 1998 and references therein).

This will be the lower limit of ^{56}Ni mass, as the bolometric curve for SN 2004et does not include contribution from near-infra-red region.

The mean nickel mass derived using the V band magnitudes in the nebular phase and steepness parameter S is $0.06 \pm 0.02 M_{\odot}$.

Chugai (1990) and Elmhamdi, Chugai & Danziger (2003) find that the $\text{H}\alpha$ luminosity at the nebular phase can be used to estimate the nickel mass. The $\text{H}\alpha$ luminosity is found to be proportional to ^{56}Ni mass during 200-400 days after the explosion. Comparing the $\text{H}\alpha$ luminosity of SN 2004et around day 250 (ref. Fig. 8 top panel) with that of SN 1987A during the same phase, it is found that the $\text{H}\alpha$ luminosities in both SNe are similar. Assuming the mass, energy and mixing conditions do not vary strongly, this indicates the nickel mass in SN 2004et to be similar to that estimated for SN 1987A. This is consistent with the photometric estimates.

6 DUST FORMATION IN THE EJECTA

The formation of dust in the supernova ejecta increases the rate of decline of the optical, especially the V band, light curve, as the optical light is reprocessed by the dust and an excess emission in IR is observed. Further, dust formation in the inner envelope of the supernova ejecta shifts the peak of the optical and infrared emission lines towards blue, due to a preferential extinction of the redshifted edge of the emission lines by the dust (Lucy et al. 1991). The signature of dust formation was seen in SN 1987A (Danziger et al. 1991) and SN 1999em (Elmhamdi et al. 2003) as an observable blueshift in the emission peaks of the [OI] doublet components, beyond ~ 400 days. It should be noted that both SNe showed an early blueshift ($\sim 200 - 300$ days) in the [OI] component, probably as a result of superposition of the blend of Fe II lines (multiplet 74).

Fig. 11 shows the temporal evolution of the $\text{H}\alpha$ and [O I] 6300, 6364 Å line profiles during 277–465 days. A blueshift in the emission peak is clearly seen beyond day 300 in both lines. Further, the $\text{H}\alpha$ line shows a clear flattening of the emission peak. The blueshift in the emission peak and the flattening were seen in both SN 1987A and SN 1999em during the dust formation epoch. The absence of any ‘blue bump’ in the [OI] line due to Fe II 6250 Å feature (ref. Fig. 11, top panel) indicates that the observed blue shift in the emission peak is not due to a blending of Fe II lines, and more likely due to dust formation.

It is evident from Fig. 3 that the decline rate of the light curve of SN 2004et in the V

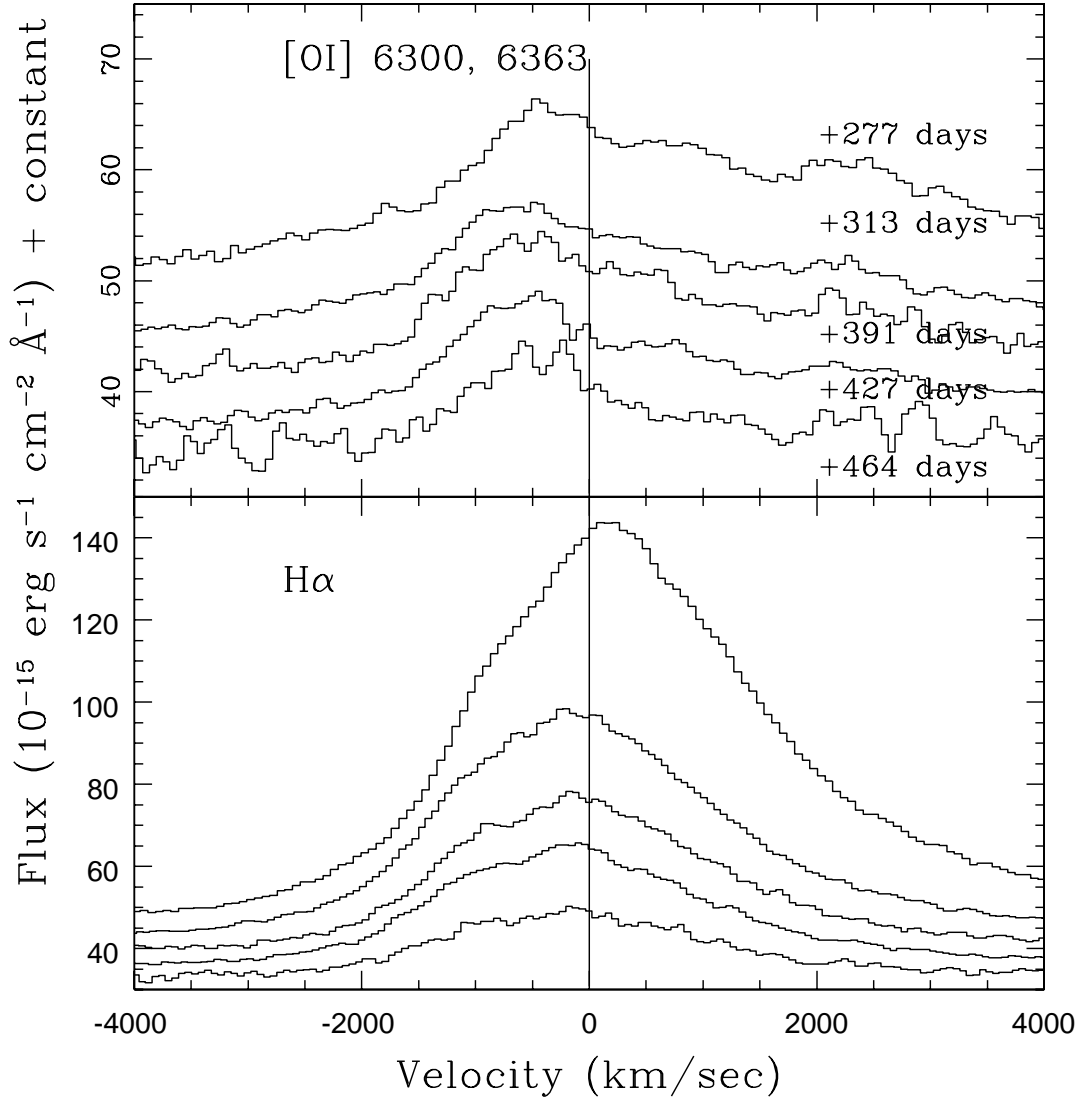


Figure 11. Temporal evolution of line profile of oxygen doublet [OI] 6300, 6364 Å (top panel) and H α (bottom panel). The vertical line corresponds to the zero velocity of the [OI] 6300 Å and H α . The epochs are as marked for the [OI] profile.

band starts steepening ~ 320 days after the explosion. A similar effect was seen in both SN 1987A and SN 1999em during dust formation. It should, however, be noted here that dust formation occurred at much later phases, beyond day 400 in both these SNe.

The evolution of the emission line profiles together with the steepening of the light curve beyond day ~ 320 suggest an early dust formation in the case of SN 2004et.

7 PROGENITOR STAR PROPERTIES

The supernova outburst properties depend on three basic parameters: the mass M of the envelope that is ejected, the radius R of the star prior to the outburst and the energy E of explosion. An analysis of supernova light curve combined with the spectroscopic evolution allows the derivation of these important parameters. With the help of hydrodynamic models of SNe IIP, Litvinova & Nadyozhin (1985) derived expressions for these parameters in terms of the observable parameters, namely, the length of the plateau Δt , the absolute magnitude M_V at the midpoint of the plateau and the velocity of photosphere U_{ph} at mid plateau.

The light curve of SN 2004et indicates the length of the plateau to be $\Delta t = 120 \pm 10$ days. The absolute magnitude at mid plateau is $M_V = -17.14$ mag. The weak iron lines indicate a mid plateau velocity $U_{ph} = 3560 \pm 100$ km sec⁻¹. Using these values and the relations given by Litvinova & Nadyozhin (1985) we estimate the explosion energy $E_{\text{exp}} = 1.20_{-0.3}^{+0.4} \times 10^{51}$ ergs.

The luminosity of [OI] doublet ~ 1 yr after the explosion is powered by the γ -ray deposition and by ultraviolet emission arising from the deposition of γ -rays in oxygen-poor material. The [OI] doublet luminosity is related to the mass of oxygen, the ‘excited’ mass in which the bulk of the radioactive energy is deposited and the efficiency of transformation of the energy deposited in oxygen into the [OI] luminosity. The [OI] luminosity in SN 1987A implies an oxygen mass in the range $1.5 - 2 M_{\odot}$. The fact that derived [OI] luminosity for SN 2004et before dust formation is comparable to that of SN 1987A at similar epochs implies similar oxygen mass in SN 2004et also. The nucleosynthesis computations (Chugai 1994, Woosley & Weaver 1995) indicate that this oxygen mass corresponds to a main-sequence stellar mass of $20 M_{\odot}$. An analysis of the radio light curve of SN 2004et by Chevalier, Fransson & Nymark (2006) indicates a mass loss rate for the progenitor that suggests a mass of $20 M_{\odot}$, similar to the estimate based on a comparison of the [OI] luminosity with that of SN 1987A. However, Li et al. (2005) estimate the progenitor mass to be $\sim 15 M_{\odot}$ and also the progenitor to be a yellow supergiant.

8 SUMMARY

We have presented *UBVRI* photometric and spectroscopic data for SN 2004et from ~ 8 until ~ 541 days after the explosion. The shape of the light curve as well as the spectral evolution indicate that it is Type IIP supernova, which was caught young, soon after the

shock breakout. SN 2004et reached maximum in B band on JD 2453280.90, ~ 10 days after the explosion. The luminosity at maximum indicates SN 2004et to be at the brighter end of SNe IIP. The late phase photometry indicates that the decline rate of light curve during $\sim 180 - 300$ d was similar to the ^{56}Co to ^{56}Fe radioactive decay, while it was significantly faster beyond ~ 320 d.

The spectra of SN 2004et in early phase shows an $\text{H}\alpha$ profile that is emission dominated with P-Cygni profile that is shallower than other SNe IIP. The velocity evolution of SN 2004et determined using the weak iron lines is similar to other well studied SNe IIP, although the photospheric velocity in SN 2004et was higher than other SNe IIP at all epochs. The $\text{H}\alpha$ line indicates the presence of a high velocity component in the early phases, with the velocity of this component being ~ 7000 km sec $^{-1}$ higher than the normal component.

The mass of ^{56}Ni synthesized during the explosion is estimated to be $0.06 \pm 0.02 M_{\odot}$.

The $\text{H}\alpha$ and [OI] 6300, 6364 Å line profile evolution beyond day 320, and the steepening of the V light curve at the same epoch is interpreted as an effect of an early dust formation.

The brightness of the plateau, its duration and the expansion velocity of the supernova at the middle of the plateau is used to estimate the explosion energy $E_{exp} = 1.20_{-0.30}^{+0.38} \times 10^{51}$ ergs. The main-sequence mass of the progenitor based on [OI] luminosity is estimated to be $20 M_{\odot}$.

ACKNOWLEDGEMENTS

We thank the anonymous referee for useful comments, which helped in improving the manuscript. We thank all the observers of the 2-m HCT who kindly provided part of their observing time for the supernova observations. We also thank Jessy Jose and S. Ramya for their help during observations. This work has made use of the NASA Astrophysics Data System and the NASA/IPAC Extragalactic Database (NED) which is operated by Jet Propulsion Laboratory, California Institute of Technology, under contract with the National Aeronautics and Space Administration.

REFERENCES

- Barbon R., Benetti S., Rosino L., Cappellaro E., Turatto M., *A&A*, 237, 79.
 Baron R., Ciatti F., Rosino L., 1979, *A&A*, 72, 287.

- Baron E., Branch D., Hauschildt P.H., Filippenko A.V., Kirshner R.P., Challis P.M., Jha S., Chevalier R., Fransson C. et al., 2000, *ApJ*, 545, 444.
- Benetti S., Cappellaro E., Turatto M., Della Valle M., Mazzali P., Gouiffes C., 1994, *A&A* 285, 147.
- Benetti S., Turatto M., Balberg S., Zampieri L., Shapiro S.L., Cappellaro E., Nomoto K., Nakamura T., Mazzali P., Patat F., 2001, *MNRAS*, 322, 361.
- Bessell M.S., 1990, *PASP*, 102, 1181.
- Bessell M.S., Castelli F., Plez B., 1998, *A&A*, 333, 231.
- Cardelli J.A., Clayton G.C., Mathis J.S., 1989, *ApJ*, 345, 245.
- Chevalier R.A., Fransson C., Nymark T.K., 2006, *ApJ*, 641, 1029.
- Chugai N.N., 1990, *SvAL*, 16, 457.
- Chugai N.N., 1994, *ApJ*, 428, L17.
- Danziger I.J., Lucy L.B., Bouchet P., Gouiffes C., 1991 in *Supernovae*, eds. Woosley S.E., New York, Springer, p69.
- Elmhamdi A., Chugai N.N., Danziger I.J., 2003, *A&A* 404, 1077
- Elmhamdi A., Danziger I.J., Chugai N., Pastorello A., Turatto M., Cappellaro E., Altavilla G., Benetti S., Patat F., Salvo M., 2003, *MNRAS*, 338, 939.
- Filippenko A.V., Foley, R.J., Treu, T., Malkan, M. A., 2004, *IAU Circ.* 8414.
- Hamuy M., 2003, *ApJ*, 582, 905.
- Hamuy M., Pinto P.A., 2002, *ApJL*, 566, L63.
- Hamuy M., Suntzeff N.B., Gonzalez R. Martin G., 1988, *AJ*, 95, 63.
- Hamuy M., Pinto P.A., Maza J., Suntzeff N.B., Phillips M.M., Smith R.C., Corbally C.J., Burstein D., Li Y., 2001, *ApJ*, 558, 615.
- Hendry M.A., Smart S.J., Maund J.R., Pastorello A., Zampieri L., Benetti S., Turatto M., Cappellaro E, Meikle W.P.S. et al., 2005, *MNRAS*, 359, 906.
- Landolt A.U., 1992, *AJ*, 104, 340
- Leonard D.C., Filippenko A.V., Gates E.L., Li W., Eastman R.G., Barth A.J., Bus S.J., Chornock R., et al. 2002a, *PASP*, 114, 35.
- Leonard D.C., Filippenko A.V., Li W., Matheson T., Kirshner R.P., Chornock R., Van Dyk S.D., Berlind P., et al., 2002b, *AJ*, 124, 2490.
- Leonard D.C., Kanbur S.M., Ngeow C.C., Tanvir N.R., 2003, *ApJ*, 594, 247.
- Li Weidong, Filippenko, A.V., and Van Dyk S.D., 2005, *Astronomer's Telegram (ATel)* 492
- Li Weidong, Van Dyk S.D., Filippenko, A.V., and Cuillandre Jean-Charles, 2005, *PASP*,

117, 121.

Li Weidong, Van Dyk S.D., Filippenko A.V., Cuillandre J., Jha S., Bloom J.S., Riess A.G., Livio M., 2006, *ApJ*, 641, 1060.

Litvinova Y., Nadyozhin D.K., 1985, *Sov. Astron. Lett*, 11, 45.

Lucy L.B., Danziger I.J., Gouiffes C., Bouchet P., 1991 in *SANTA CRUZ*, p82.

Nugent P., Sullivan M., Ellis R., Gal-Yam A., Leonard D.C., Howell D.A., Astier P., Carlberg R.G., 2006, *astro-ph/0603535*.

Patat F., Baron R., Cappallaro E., Turatto M., 1994, *A&A*, 282, 731

Pierce M.J., 1994, *ApJ*, 430, 53

Sandage A., Tammann G.A., 1981, *Revised Shapley-Ames Catalog of Bright Galaxies*

Schlegel D.J., Finkbeiner D.P., Davis M., 1998, *ApJ*, 500, 525

Schmidt B.P., Krishna R.P., Eastman R.G., 1992, *ApJ*, 395, 366.

Schmidt B.P., Krishna R.P., Schild R., Leibundgut B., Jeffery D., Willner S.P., Peletier R., Zabludoff A.I. et al., 1993, *AJ*, 105, 2236

Schmidt B.P., Krishna R.P., Eastman R.G., Phillips M.M., Suntzeff N.B., Hamuy M., Maza J., Aviles R., 1994, *ApJ*, 432, 42.

Schoniger F., Sofue Y., 1994, *A&A*, 283, 21.

Smartt S.J., Maund J.R., Hendry M.A., Tout C.A., Gilmore G.F., Mattila S., Benn C.R., 2004, *Sci.*, 303, 499.

Stockdale C.J., Weiler, K.W., Van Dyk, S.D., Sramek, R.A., Panagia, N., and Marcaide, J.M., 2004, *IAU Circ.*, 8415.

Suntzeff N.B., Bouchet P., 1990, *AJ*, 99, 650.

Turatto M., Mazzali P. A., Young T. R., Nomoto K., Iwamoto K., Benetti S., Cappallaro E., Danziger I. J. et al., 1998, *ApJL*, 498, L129.

Van Dyk S.D., Li W., Filippenko A.V., 2003 *PASP*, 115, 1289.

Woosley S.E., Weaver T.A., 1995, *ApJS*, 101, 181

Zwitter T., Munari U., Moretti S., 2004, *IAU Circ.* 8413, 1.